

# A semi-empirical effective medium theory for metals and alloys

K.W. Jacobsen, P. Stoltze, J.K. Nørskov\*

*Center for Atomic-Scale Materials Physics, Physics Department, Technical University of Denmark, DK-2800 Lyngby, Denmark*

Received 2 January 1996; accepted for publication 10 May 1996

## Abstract

A detailed derivation of the simplest form of the effective medium theory for bonding in metallic systems is presented, and parameters for the fcc metals Ni, Pd, Pt, Cu, Ag and Au are given. The derivation of parameters is discussed in detail to show how new parameterizations can be made. The method and the parameterization is tested for a number of surface and bulk problems. In particular we present calculations of the energetics of metal atoms deposited on metal surfaces. The calculated energies include heats of adsorption, energies of overlayers, both pseudomorphic and relaxed, as well as energies of atoms alloyed into the first surface layer.

**Keywords:** Construction and use of effective interatomic interactions; Metal–metal nonmagnetic heterostructures; Single crystal epitaxy

## 1. Introduction

Rapid advances in methods for total energy calculations based on density functional theory have made it possible to study the energetics and in some cases even the molecular dynamics over short time intervals of hundreds of atoms with a very high accuracy. This is sufficient for many problems, but there are numerous others in solid state physics, surface science and materials science where systems of this size are far too small or the possible time scales too short to expose the relevant effects. This points to the need for simpler methods with a reasonable accuracy. Such methods may also be valuable when one is interested in trying out ideas or in constructing simplified (qualitative) models.

In recent years a class of simplified models has been introduced which is generally found to describe the fcc metals quite well. The new feature

of these methods is that they include some many-atom interactions. The interactions between any two atoms depend in general not only on their mutual distance but also on the number, kind, and position of the surrounding atoms. These methods are based on the effective medium [1] or quasi-atom [2] concept of an electron density or local volume-dependent contribution to the total energy, and go under names like the effective medium theory [3,4], the embedded atom method [5], the glue model [7] or the corrected effective medium theory [8]. The Finnis–Sinclair method [6], which is based on a tight-binding approach, also includes many-atom interactions in a similar way. Most of these approaches assume a functional form for the interactions and then fit the parameters to available experimental information. In the effective medium approaches [3,8] on the other hand, some or most of the parameters have been calculated within the local density approximation.

The purpose of the present paper is to present a consistent set of parameters for the simplest

\* Corresponding author. e-mail: nørskov@fysik.dtu.dk

effective medium description of the six fcc metals Cu, Ag, Au, Ni, Pd, Pt and their alloys. The present parameterization gives a single set of parameters per element describing the interaction of this element with itself and all the others. The present parameterization is built upon three sets of input: some parameters are determined from the electron densities obtained from self-consistent calculations for the atoms embedded in a homogeneous electron gas. Other parameters are fitted to give the experimental cohesive energies, lattice constants and elastic constants of the elemental metals [28]. Finally, we derive the last parameter for each element from a database for alloy heats of formation. The set of parameters derived here gives a reasonable overall description of the systems for which it is derived, including trends in surface energies, reconstructions, diffusion barriers, alloy heats of formation, surface alloying, etc., but the absolute accuracy is of course limited for such an approximate theory. An additional purpose of the present paper is to show how the parameterization is done, so that it is possible to construct new parameterizations that describe the details of a specific system better, possibly at the expense of the overall quality of the parameter set for all the metal combinations.

In the following we first give a derivation of the effective medium theory in its simplest form. We will show how most parameters can be obtained analytically without extensive fitting procedures. In the following section we give a few examples of applications of the present parameterization which illustrate the strengths and weaknesses of the approach. The main application is a set of calculations of the energetics of Cu deposited on Cu(111) and Au and Ag deposited on the (111), (100), and (110) surfaces of Ni. We show that information about the structure, energetics and aspects of the kinetics of these systems can be obtained which is in excellent agreement with experiment.

## 2. Theory

The basic idea of the effective medium theory is to calculate the energy of an atom in an arbitrary environment by first calculating it in some properly

chosen reference system, the effective medium, and then estimate the energy difference between the real system and the reference system. We write the total energy of the system

$$E = \sum_i E_{c,i} + (E - \sum_i E_{c,i}), \quad (1)$$

where  $E_{c,i}$  is the energy of atom  $i$  in the reference system. The essence of the method is then to choose the reference system so close to the real system that the correction  $E - \sum_i E_{c,i}$  is small enough that it can be estimated using perturbation theory or some other approximate form. Another important feature is that the reference system is chosen so that the binding energy of the atom in the reference system is easily obtained.

The link between the real system and the reference system is a single parameter which determines how an atom in the real system is mapped onto a reference system. The original choice of reference system has been the homogeneous electron gas [1,3]. The energy  $E_{c,i}$  is then the energy of atom  $i$  in a homogeneous electron gas, and the density of the electron gas is chosen to be given by the average electron density around the atom in the system of interest. Other choices are of course possible [8]; in the present paper we shall be using the perfect fcc crystal as the reference system. The lattice constant of the crystal can be varied to approximate the environment of the atom in the real system as closely as possible. In analogy with the case where the reference system is the homogeneous electron gas, this is obtained by adjusting the lattice constant so that the atom in the fcc crystal is surrounded by the same average electron density as in the real system. This ensures that the screening is approximately the same in the two systems.

In a series of papers we have shown how to derive the form of the correction term  $E - \sum_i E_{c,i}$  in Eq. (1) from density functional theory [3,9]. The total energy of the systems can be written

$$E = \sum_i E_{c,i}(n_i) + \Delta E_{AS} + \Delta E_{1el}, \quad (2)$$

where  $E_c$ ,  $\Delta E_{AS}$  and  $\Delta E_{1el}$  are called the cohesive function, atomic-sphere correction, and one-electron correction, respectively. The atomic-sphere correction is the difference in electrostatic and exchange-correlation energy for the atoms in

the system of interest and in the reference system. It can be approximated very well by a difference of pair interaction energies in the two systems [9]. The last term is the difference in the sum of one-electron energies in the two systems. These terms can be calculated ab initio without any input from experiment for both metals and semiconductors [9]. While such an approach gives an accuracy comparable to self-consistent calculations, it involves an LMTO tight-binding calculation of the one-electron energy difference, and this is quite computer intensive.

If the one-electron energy is small and can be neglected, a pair-potential approximation for the atomic sphere correction leads to an expression for the total energy of the form

$$E = \sum_i [E_{c,i}(n_i) + \Delta E_{AS}(i)] \quad (3)$$

$$= \sum_i \left\{ E_{c,i}(n_i) + \frac{1}{2} \left[ \sum_{j \neq i} V_{ij}(r_{ij}) - \sum_{j \neq i}^{\text{ref}} V_{ij}(r_{ij}) \right] \right\}. \quad (4)$$

A direct evaluation of  $\Delta E_{AS}$  and  $\Delta E_{1el}$  shows that the latter is not necessarily small, even for simple metals. We shall use a pair-potential approximation for the one-electron energy, and this is included in the total energy expression through an adjustment of the potential  $V_{ij}$  in the atomic sphere correction. However, in the following we shall refer to the pair-potential as just the atomic sphere correction.

We stress that Eq. (4) is very far from a simple pair-interaction model. We are only using pair interactions to describe the difference in energy between two very similar systems.

### 2.1. The total energy expression

In the following we shall give a complete description of the implementation of Eq. (4) to describe the energetics of a solid. This implies a description of how to get the density arguments, the cohesive energy function and the pair potentials. We begin by considering a one-component system, where all the atoms have the same nuclear charge  $Z$ . We shall also for simplicity first limit ourselves to an effective nearest-neighbor model.

First, we consider the density argument  $n_i$  of the cohesive function  $E_c(n_i)$ . This is the parameter which connects the surroundings of atom  $i$  in the system of interest to the reference system of atom  $i$ . The embedding density  $n_i$  of atom  $i$  is calculated by superimposing density contributions from the neighboring atoms:

$$n_i = \sum_{j \neq i} \Delta n_j(s_i, r_{ij}), \quad (5)$$

where we assume that the density tail  $\Delta n(s, r)$  from a neighboring atom a distance  $r$  away and averaged over a sphere with radius  $s$  around atom  $i$  has an exponential form

$$\Delta n(s, r) = \Delta n_0 \exp[\eta_1(s - s_0) - \eta_2(r - \beta s_0)]. \quad (6)$$

The sphere radius  $s_i$  is chosen so that the total charge within the sphere is zero (neutral sphere). In the fcc reference system the neutral sphere is to a very good approximation the same as the Wigner–Seitz sphere which is easily related to the nearest-neighbor distance  $d_{nn}$ :  $d_{nn} = \beta s$ , where the geometric factor  $\beta$  is  $(16\pi/3)^{1/3}/\sqrt{2} \approx 1.81$ .

The electron density for each of the atoms is taken from self-consistent calculations for the atom in a homogeneous electron gas at a typical metallic electron density. It has been shown in a number of cases that a superposition of such “atom in jellium” electron densities gives excellent total energies. The reason is that the error in electron density only shows up to second order in the total energy due to the variational property of the total energy functional [3,10].

For such a set of “atom-like” electron densities, there is a one-to-one correspondence between the average electron density around a given atom and its neutral sphere radius, and it turns out that it is simpler to consider the neutral sphere radius as the parameter connecting the real and the reference systems. We therefore need a relation between the embedding density  $n$  and the neutral sphere radius  $s$ . Based on local density functional calculations this relationship has been shown to be approximately exponential [3]

$$\bar{n}(s) = n_0 \exp[-\eta(s - s_0)]. \quad (7)$$

By applying Eq. (6) to an fcc crystal of varying nearest-neighbor distance  $r = \beta s$  we see (in a nearest-neighbor model) that the prefactor  $\Delta n_0$  must

equal  $n_0/12$  and that the exponents are related by  $\beta\eta_2 = \eta + \eta_1$ .

Solving Eq. (5) we find the neutral sphere radius  $s_i$

$$s_i = s_0 - \frac{1}{\beta\eta_2} \log \left( \frac{\sigma_{1,i}}{12} \right), \quad (8)$$

$$\sigma_{1,i} = \sum_{j \neq i} \exp [-\eta_2(r_{ij} - \beta s_0)]. \quad (9)$$

Moving now to the cohesive function as a function of the neutral sphere radius  $s$ , this is simply the cohesive energy of the metal in question as a function of Wigner–Seitz radius. We choose to parameterize it using the functional form suggested by Rose et al. [11]

$$E_c(s) = E_0 f[\lambda(s - s_0)], \quad (10)$$

$$f(x) = (1 + x) \exp(-x), \quad (11)$$

where  $s_0$  is the equilibrium (zero-pressure) neutral-sphere radius.

Finally the atomic sphere correction  $\Delta E_{AS}(i)$  measuring the energy difference between the real and the reference system is written

$$\Delta E_{AS}(i) = \frac{1}{2} \left[ \sum_{j \neq i} v(r_{ij}) - 12v(\beta s_i) \right], \quad (12)$$

where we have used the fact that in the fcc reference system there are 12 nearest neighbors at a distance  $r = \beta s_i$  determined by the Wigner–Seitz radius  $s_i$ .

The pair potential is parameterized as

$$V(r) = -V_0 \exp[-\kappa(r/\beta - s_0)], \quad (13)$$

so the calculation of  $\Delta E_{AS}(i)$  involves a sum over exponential functions:

$$\sigma_{2,i} = \sum_{j \neq i} \exp \left[ -\frac{\kappa}{\beta} (r_{ij} - \beta s_0) \right]. \quad (14)$$

From the above expressions one can easily derive the following expressions for the cohesive, elastic and structural properties of the fcc metals. The cohesive energy is given by  $E_0$

$$E_{coh} = |E_0|, \quad (15)$$

the bulk modulus is given by

$$B = \frac{-E_0 \lambda^2}{12\pi s_0}, \quad (16)$$

and the shear modulus is given by

$$C_{44} = \frac{sV_0\kappa\delta}{8\pi s_0}, \quad (17)$$

where we introduce the parameter

$$\delta = \beta\eta_2 - \kappa. \quad (18)$$

As mentioned above, we take the density parameter  $n_0$  (which does not enter into the description of the pure metals) and the parameter  $\eta$  describing the fall-off of the electron density from a self-consistent calculation of the atom embedded in a homogeneous electron gas, and we have taken  $\eta_1 = 0.5a_0^{-1}$ , which is a typical value for the metals considered. Table 1 shows the calculated values for the metals considered here. The other parameters are determined from experimental properties of the metals in the following way. The equilibrium Wigner–Seitz radius  $s_0$  is given by the lattice constant and  $E_0$  is (minus) the cohesive energy. The parameter  $\lambda$  is derived from the bulk modulus using Eq. (16), and finally  $V_0\delta = V_0(\beta\eta_2 - \kappa)$  is determined from the shear modulus in Eq. (17). Only the product  $V_0\delta$  can be deduced in this way, but it turns out that for a single metal the value of the individual terms never enter separately in the case where  $\delta/\eta_2 \ll 1$ , which is the relevant range of  $\delta$ 's. (This follows from an expansion of the atomic sphere correction energy to first order in  $\delta/\eta_2$ .) In this way all necessary parameters for the potential for a pure metal have been determined.

## 2.2. Two-component metal systems

For a two component system (A,B) the energy expression is generalized as follows. For each kind of atom (identified through the nuclear charge  $Z$ ) we have a cohesive function determined by the parameters  $E_0$ ,  $\lambda$ , and  $s_0$  ( $E_{0A}$ ,  $\lambda_A$ , and  $s_{0A}$  for atoms of type A and similarly for atoms of type B). The requirement that the reference system should be determined by the embedding density now gives that the neutral radius of a type A atom is determined by

$$s_A = s_{0A} - \frac{1}{\beta\eta_{2A} + \eta_{1B} - \eta_{1A}} \log \frac{1}{12} (\sigma_{1AA} + \chi_{AB}\sigma_{1AB}), \quad (19)$$

Table 1  
EMT parameters

	$E_0$ (eV)	$s_0$ (bohr)	$V_0$ (eV)	$\eta_2$ (bohr $^{-1}$ )	$\kappa$ (bohr $^{-1}$ )	$\lambda$ (bohr $^{-1}$ )	$n_0$ (bohr $^{-3}$ )
Cu	−3.51	2.67	2.476	1.652	2.740	1.906	0.00910
Ag	−2.96	3.01	2.132	1.652	2.790	1.892	0.00547
Au	−3.80	3.00	2.321	1.674	2.873	2.182	0.00703
Ni	−4.44	2.60	3.673	1.669	2.757	1.948	0.01030
Pd	−3.90	2.87	2.773	1.818	3.107	2.155	0.00688
Pt	−5.85	2.90	4.067	1.812	3.145	2.192	0.00802

where  $\sigma_{1AA}$  is the sum Eq. (9) running over the A neighbors to the atom and  $\sigma_{1AB}$  is the sum over the B neighbors. The coefficient  $\chi_{AB}$  is given by

$$\chi_{AB} = \frac{n_{0B} e^{-\eta_{1B}s_{0B}}}{n_{0A} e^{-\eta_{1A}s_{0A}}} e^{(\eta_{1B}-\eta_{1A})(s_A-s_{0A})}. \quad (20)$$

The last exponential function contains the radius  $s_A$  in the exponent, but the exponent is usually so small that value of the exponential function can be taken to be 1. In the parametrization presented here the parameter  $\eta_1$  is the same for the different metals and this is rigorously the case. Similarly the atomic sphere correction for a type A atom is written

$$\Delta E_{AS}^A = \sum_{j_A \neq i} V_{AA}(r_{ij}) + \chi_{AB} \sum_{j_B \neq i} V_{AB}(r_{ij}) - 12V_{AA}(\beta s_{iA}). \quad (21)$$

It can be seen that no new parameters are introduced in order to describe a system with more than one type of atom. However, as discussed above it is only the product of  $\delta_A$  and  $V_{0A}$  which really enters the potential for metal A. For the alloys the separate values of the  $\delta$ 's and  $V_0$ 's become important. We therefore have one extra parameter, which is not important for the single component results, but which matters for the alloys. We have exploited this by choosing this extra parameter per metal to give a reasonable description of the alloy heats of formation for these metals.

The particular choice of the ratio of the  $\delta = \beta\eta_2 - \kappa$  and  $V_0$  parameters given in Table 1 is therefore a compromise which gives a reasonable description of the alloy heats of formation and impurity heats of solution for the six metals considered. This is illustrated in Fig. 1, where we compare the calculated heat of solution of all the metals in

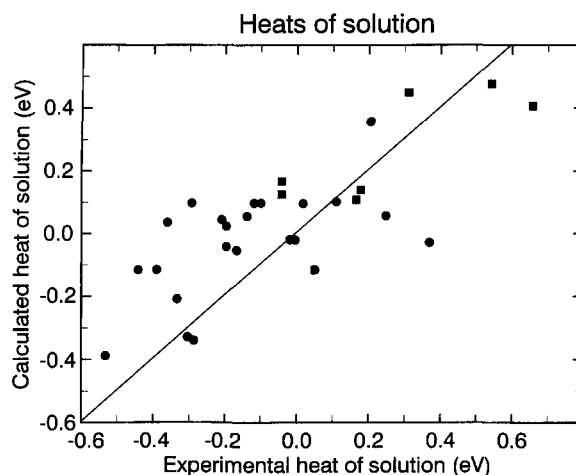


Fig. 1. Comparison of calculated and experimental heats of solution. The experimental values are from Ref. [12].

each other to experiment, where available [12]. It is seen that the present very simple model reproduces the overall trends, but the standard deviation between the experimental and the model heats of solution is considerable (0.18 eV). Half of this stems from a general tendency for more positive calculated heats of solution. When comparing two alloys, the error of each is therefore of the order 0.1 eV. This means that if we are interested in the details of a particular combination of metals it may be better to choose a ratio of  $\delta$  to  $V_0$  which best describes this particular alloy [14].

### 2.3. More than nearest neighbors

The above expressions are readily generalized to more than nearest neighbors by replacing  $\sigma_{1,i}$  by

$$\sigma_{1,i} = \frac{1}{\gamma_1} \sum_{j \neq i} \exp[-\eta_2(r_{ij} - \beta s_0)] \theta(r_{ij}), \quad (22)$$

and replacing  $\sigma_{2,i}$  by

$$\sigma_{2,i} = \frac{1}{\gamma_2} \sum_{j \neq i} \exp \left[ -\frac{\kappa}{\beta} (r_{ij} - \beta s_0) \right] \theta(r_{ij}), \quad (23)$$

where the summations now may include more than nearest neighbors. The smooth cut-off function  $\theta(r)$  is taken to have the form

$$\theta(r) = \{1 + \exp [a(r - r_c)]\}^{-1}, \quad (24)$$

where  $r_c$  is the cut-off radius and  $a$  determines the steepness of the cut-off. The normalization constants  $\gamma_1$  and  $\gamma_2$  are introduced in order to keep the properties that  $E_c = E_0$  and  $\Delta E_{AS} = 0$  in the equilibrium fcc reference system even when the summations are extended to more than nearest neighbors. Since we do not let  $\gamma_1$  and  $\gamma_2$  be density dependent, there will be a (very) small shift of the equilibrium lattice constant in the fcc structure compared to the input value for  $s_0$ .

### 3. Selected results

In the following we illustrate the strengths and weaknesses of the simplified effective medium approach described above by considering a few selected results. A large number of applications for bulk metals [13], alloy phase diagrams [14], surface melting [15,16], surface diffusion [17] and surface alloying [18] has been published, and the reader is referred to these original articles for a more detailed discussion of the physics involved. The examples chosen here are mainly taken from work already published, but a new comprehensive study of the interaction of metal atoms deposited on metal surfaces is also presented.

#### 3.1. The pure metals

For the pure metals, bulk properties like the cohesive energy, bulk modulus and shear modulus, and lattice constant are used to define the potential parameters, and are therefore very well reproduced by the model (they are not reproduced exactly because the simple analytic fitting described above was done using only nearest neighbors, while the calculations include third-nearest neighbors).

Trends in other bulk properties, like the thermal expansion coefficient or the vacancy formation energy, are also reasonably well described in the model, but there may be significant quantitative deviations from the experimental values. This can be seen from the comparisons to experiment in Table 2.

Trends in the surface energies are also reasonably described, but the absolute magnitude tends to be considerably too small (see Fig. 2). This problem can be traced back to the neglect of the one-electron correction, which cannot be accurately described as a pair-potential difference at the surface. Energy differences involved in for example, reconstructions tend to be better described. In Fig. 3 we show the calculated energy involved in forming the  $(1 \times 2)$  missing-row reconstruction of the (110) surfaces of the six metals. The model correctly predicts an increasing tendency towards reconstruction down through the periodic table. It is known experimentally that Pt and Au(110) exhibit a  $(1 \times 2)$  missing-row reconstruction while Cu, Ni and Ag do not [21]. Pd is predicted in the model to reconstruct in contradiction to experiment. The Pd(110) surface is, however, known to be highly unstable towards disordering [22]. Even the absolute magnitude of the reconstruction energy for Au is reasonable compared to full local density functional calculations [23].

These examples illustrate that trends generally seem to be reasonably described, while absolute energies may be underestimated quite substantially, in particular for low-coordinated systems.

Table 2

Comparison of the calculated ( $H_{\text{vac}}^{\text{emt}}$ ) and experimental ( $H_{\text{vac}}^{\text{exp}}$ ) vacancy-formation energies and thermal expansion coefficients  $\alpha$ ; the experimental values are from Ref. [19]

	$H_{\text{vac}}^{\text{emt}}$ (eV)	$H_{\text{vac}}^{\text{exp}}$ (eV)	$\alpha^{\text{emt}}$ (ppm K <sup>-1</sup> )	$\alpha^{\text{exp}}$ (ppm K <sup>-1</sup> )
Cu	1.2	1.3	22	17
Ag	0.9	1.1	32	19
Au	0.7	0.9	18	14
Ni	1.9	1.7	15	14
Pd	0.9	1.5	24	11
Pt	1.0	1.6	17	9

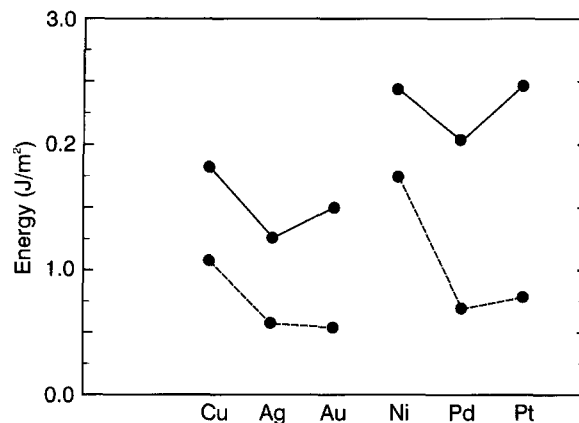


Fig. 2. Comparison of the calculated surface energies of the (111) surfaces (dashed) with values deduced from experiment [20] (full curves).

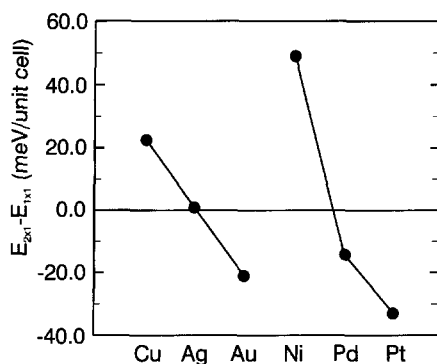


Fig. 3. Calculated energy difference between the  $(1 \times 2)$  missing-row reconstructed and the reconstructed (110) surfaces. A negative energy difference means that the reconstructed surface is the most stable. The energies are per  $(1 \times 2)$  unit cell.

### 3.2. Alloys and their surfaces

In simulations of the growth of one metal on another or of the segregation of a metallic component out of an alloy, it is important to know the solution energy of a metal atom as a function of its position relative to the surface.

When a metal is deposited on another metal with a different lattice constant, the overlayer may take the substrate inter-atomic distance and grow pseudomorphically, or it may keep its interatomic distances. In Fig. 4 we show the energy of an Ag overlayer on Cu(111) as a function of the ratio of the overlayer to the substrate unit-cell size. The model is seen to suggest that a Moire pattern

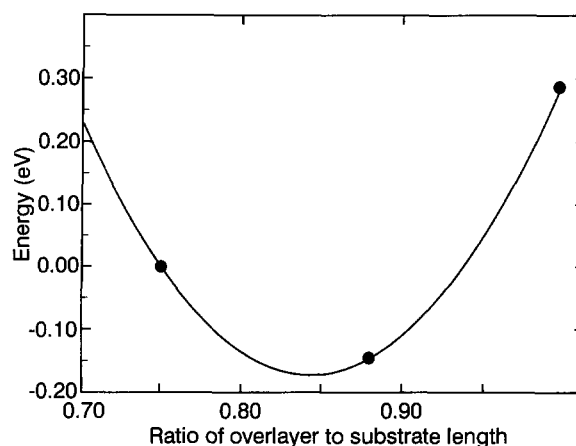


Fig. 4. Calculated energy of an Ag overlayer on a Cu(111) surface as a function of the ratio of the number of overlayer atoms to the number of substrate atoms per unit length.

should evolve with a ratio of the overlayer-to-substrate lattice constant of around 0.85. Experimentally, deposition of Ag onto Cu(111) at low temperature gives rise to such a Moire pattern with an overlayer-to-substrate length ratio of 0.89 [27]. The overlayer is also found experimentally to be slightly rotated with respect to the substrate. We have not looked into this possibility in the present calculations.

The experimental situation is often even more complicated due to both mixing between the first and second layers (see later) and the formation of new structures due to the misfit (misfit dislocations)

[24–26]. The overlayer structure for the Ag/Cu(111) system is thus only expected at low temperatures, where other processes are frozen out [27].

We can use the present simple model to study whether an atom deposited on a surface from the gas phase will nucleate into an overlayer or will alloy into the first surface layer. We compare the energy of the overlayer structure  $E_{\text{over}}$  (at the ratio of overlayer-to-substrate density which gives the minimum energy, cf. Fig. 4) and with the energy  $E_{\text{1st}}$  of the overlayer atoms dissolved in the first layer (all energies are relative to the bulk cohesive energy). This tells us whether atoms deposited from the gas phase prefers to nucleate into islands ( $E_{\text{over}}$  gives the energy per deposited atom for large islands) or alloy into the first layer, while the substrate atoms that are expelled move to a kink on a step (where the net result is to create a new bulk atom; the number of kink and step atoms stays constant). A comparison for Au on the three faces of Ni is shown in Fig. 5. Fig. 5 shows that for the (100) and the (110) surfaces the surface alloy is considerably more stable than the overlayer. On the (111) surface the energies of the two states are the same, to within 20 meV. In such a case entropy effects will favor the disordered alloy relative to the segregated overlayer structure at

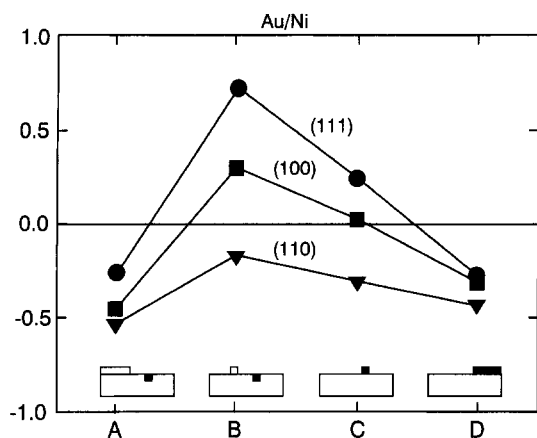


Fig. 5. Different energies for an Au atom on an Ni surface. From right to left we have Au atoms in a large Au island, an isolated Au adatom, an Ni adatom and an Au atom alloyed into the first Ni layer, and finally an Au atom in the Ni layer and an Ni atom in a large Ni island.

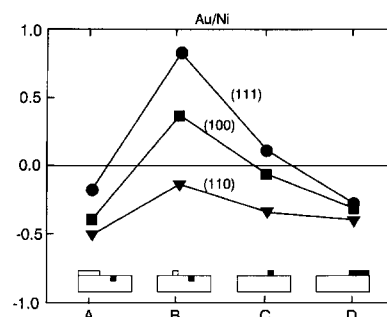


Fig. 6. Different energies for an Ag atom on an Ni surface. From right to left we have Ag atoms in a large Ag island, an isolated Ag adatom, an Ni adatom and an Au atom alloyed into the first Ni layer, and finally an Ag atom in the Ni layer and an Ni atom in a large Ni island.

room temperature. This is also what has been observed experimentally [18,24]. The alloying of Au into the first layer of Ni is a surprising result. Both experiment and the calculations show that Au and Ni do not mix in the bulk. A new two-dimensional surface alloy therefore exists for this system with properties that do not resemble the bulk alloy at all [27].

Fig. 5 also contains some information about the kinetics of the alloying process. When the Au atoms are deposited from the gas phase, they will diffuse around on the surface and may meet other Au atoms or islands and attach to them. Fig. 5 shows how the adatom will get a much lower energy by doing so. The adatom may also do an exchange with an Ni atom in the surface. Even if the Au atom first attaches to a Au island it will have to dissociate from the island again and make the exchange process in order to reach the surface alloy. The situation where the Au atom is embedded in the surface and a single Ni atom is left on the surface has a very high energy. When the Ni atoms that are ejected from the surface by the Au finally agglomerate into large islands the energy is considerably lowered. The highest energy intermediate in this chain of events is the situation just after the Ni has been ejected from the surface. This energy is by far the largest for the (111) surface and we would expect this to manifest itself in a lower rate of alloying in this case. This is what is observed experimentally. While alloying occurs at room temperature for the (110) surface [18]



annealing is necessary to accomplish the same on Ni(111) [24].

For the Ag/Ni(111) system, the picture is pretty much the same (see Fig. 6), with one exception. On the (111) surface the surface alloy has a considerably higher energy than the Ag island on top of the Ni(111) surface. This is also in agreement with experimental observations [27].

#### 4. Concluding remarks

In this paper, we have discussed in detail the simplest effective medium approach to bonding in metals and alloys. We have shown how the parameters entering the theory have been derived. The parameters have been shown to give a reasonable overall description of the six fcc metals Cu, Ag, Au, Ni, Pd, Pt and their alloys. At the detailed level the heats of solution may be off by 0.1–0.2 eV and surface energies appear to be underestimated, but trends are usually well described. We have shown how new parameters may be derived for a particular combination of metals which may describe this system better, possibly at the expense of the overall description of all the metals.

We have also presented extensive calculations of the energetics of one metal on top of another. The results give confidence that the present method may be useful as a first simple approach to an understanding of heteroepitaxy including surface alloying.

#### Acknowledgements

Many stimulating discussions with F. Besenbacher, C. Engdahl, L. Pleth Nielsen, P. Sprunger and I. Stensgaard are gratefully acknowledged. The Center for Atomic-Scale Materials Physics is sponsored by the Danish National Research Foundation.

#### References

- [1] J.K. Nørskov and N.D. Lang, Phys. Rev. B 21 (1980) 2131.
- [2] M.J. Stott and E. Zaremba, Phys. Rev. B 22 (1980) 1564.
- [3] K.W. Jacobsen, J.K. Nørskov and M. Puska, Phys. Rev. B 35 (1987) 7423; K.W. Jacobsen, Comments Condens. Matter Phys. 14 (1988) 129.
- [4] H. Häkkinen and M. Manninen, J. Phys.: Condens. Matter 1 (1989) 9765.
- [5] M.S. Daw and M.I. Baskes, Phys. Rev. Lett. 50 (1983) 1285; S.M. Foiles, M.I. Baskes and M.S. Daw, Phys. Rev. B 33 (1986) 7983; R.A. Johnson, Phys. Rev. B 39 (1989) 12554.
- [6] M.W. Finnis and J.E. Sinclair, Philos. Mag. A 50 (1984) 45.
- [7] F. Ercolessi, E. Tosatti and M. Parinello, Phys. Rev. Lett. 57 (1986) 719.
- [8] S.B. Sinnott, M.S. Stave, T.J. Raeker and A.E. DePristo, Phys. Rev. B 44 (1991) 8927.
- [9] N. Chetty, K. Stokbro, K.W. Jacobsen and J.K. Nørskov, Phys. Rev. B 46 (1992) 3798.
- [10] N. Chetty, K.W. Jacobsen and J.K. Nørskov, J. Phys. C 3 (1991) 5437.
- [11] J.H. Rose, J. Ferrante and J.R. Smith, Phys. Rev. Lett. 47 (1981) 675.
- [12] On overview with detailed references can be found in F.R. de Boer, R. Boom, W.C.M. Mattens, A.R. Miedema and A.K. Niessen, Cohesion in Metals (North-Holland, Amsterdam, 1988).
- [13] P. Stoltze, J. Phys.: Condens. Matter 6 (1994) 9495.
- [14] B. Chakraborty, Z.G. Xi, K.W. Jacobsen and J.K. Nørskov, J. Phys.: Condens. Matter 4 (1992) 7191.
- [15] P. Stoltze, J.K. Nørskov and U. Landman, Phys. Rev. Lett. 61 (1988) 440.
- [16] H. Häkkinen and M. Manninen, Phys. Rev. B 46 (1992) 1725.
- [17] J. Jacobsen, K.W. Jacobsen and J.K. Nørskov, Phys. Rev. Lett. 74 (1995) 2295.
- [18] L. Pleth Nielsen, F. Besenbacher, I. Stensgaard, E. Lægsgaard, C. Engdahl, P. Stoltze, K.W. Jacobsen and J.K. Nørskov, Phys. Rev. Lett. 71 (1993) 754; C. Engdahl, P. Stoltze, K.W. Jacobsen, J.K. Nørskov, H.L. Skriver and M. Aldén, J. Vac. Sci. Technol. A 12 (1994) 1787.
- [19] J. Emsley, The Elements (Clarendon, Oxford, 1991).
- [20] F.R. de Boer, R. Boom, W.C.M. Mattens, A.R. Miedema and A.K. Niessen, Cohesion in Metals (North-Holland, Amsterdam, 1988); H. Skriver and N. Rosengaard, Phys. Rev. B 46 (1992) 7157.
- [21] For a review, see K. Heinz, Surf. Sci. 299/300 (1994) 433.
- [22] F.M. Francis and N. Richardson, Phys. Rev. B 33 (1986) 662.
- [23] K.M. Ho and K.P. Bohnen, Europhys. Lett. 4 (1987) 345.
- [24] J. Jacobsen, L.P. Nielsen, F. Besenbacher, I. Stensgaard, E. Lægsgaard, T. Rasmussen, K.W. Jacobsen and J.K. Nørskov, Phys. Rev. Lett. 75 (1995) 489.
- [25] G.O. Pötschke and R.J. Behm, Phys. Rev. B 44 (1991) 1442.
- [26] H. Brune, H. Röder, C. Bogano and K. Kern, Phys. Rev. B 49 (1994) 2997.
- [27] P. Sprunger and F. Besenbacher, private communication.
- [28] The present parametrization differs from earlier EMT versions by relying more on experimental input.